
Article:
Abbas, SZ orcid.org/0000-0002-8783-8572, Dupont, V orcid.org/0000-0002-3750-0266 and Mahmud, T orcid.org/0000-0002-6502-907X (2019) Modelling of H2 production via sorption enhanced steam methane reforming at reduced pressures for small scale applications. International Journal of Hydrogen Energy, 4 (3). pp. 1505-1513. ISSN 0360-3199

https://doi.org/10.1016/j.ijhydene.2018.11.169

Modelling of H_2 production via sorption enhanced steam methane reforming at reduced pressures for small scale applications

S. Z. Abbas[a*], V. Dupont[b], T. Mahmud[b]

[a] Chemical Engineering Department, University of Engineering and Technology Lahore, Pakistan

[b] School of Chemical and Process Engineering, University of Leeds, LS2 9JT, UK

ABSTRACT

The production of H_2 via sorption enhanced steam reforming (SE-SMR) of CH_4 using 18 wt. % Ni/ Al_2O_3 catalyst and CaO as a CO_2-sorbent was simulated for an adiabatic packed bed reactor at the reduced pressures typical of small and medium scale gas producers and H_2 end users. To investigate the behaviour of reactor model along the axial direction, the mass, energy and momentum balance equations were incorporated in the gPROMS modelbuilder®. The effect of operating conditions such as temperature, pressure, steam to carbon ration (S/C) and gas mass flow velocity (G_s) was studied under the low-pressure conditions (2 – 7 bar). Independent equilibrium based software, chemical equilibrium with application (CEA), was used to compare the simulation results with the equilibrium data. A good agreement was obtained in terms of CH_4 conversion, H_2 yield (wt. % of CH_4 feed), purity of H_2 and CO_2 capture for the lowest (G_s) representing conditions close to equilibrium under a range of operating temperatures pressures, feed steam to carbon ratio. At G_s of 3.5 kg $m^{-2}s^{-1}$, 3 bar, 923 K and S/C of 3, CH_4 conversion and H_2 purity were up to 89% and 86% respectively compared to 44% and 63% in the conventional reforming process.

Keywords: Mathematical modelling; Sorption enhanced steam methane reforming; Simulation; Equilibrium

*Corresponding Author

Tel.: +92-3338340323

E-mail address: szabbas@uet.edu.pk

1. Introduction

The production of H_2 is one of the rapid mounting industrial processes in the recent past. According to H_2 economy report, the production of H_2 in 2004 was around 50 million tons, equivalent to 170 million tons of petroleum. The rate of increase in the production of H_2 is 10%/year [1]. The conventional steam methane reforming (SMR) process is one of the most well-known and commonly used industrial processes for the production of H_2. It contributes about 40% of the total world's production of H_2 [2-5]. The overall SMR process is endothermic in nature (+165 kJ/mol_{CH4}) and this makes it operate at high temperature conditions (700 – 1000 °C). In industrial SMR processes, CO-shift reactors are essential downstream of the reformer to convert the undesired CO and steam into CO_2 and H_2 product. Later on, amine scrubbing or pressure swing adsorption (PSA) are needed to achieve the higher purity of H_2 [6].

The rise in the demand of H_2 caused a negative impact on the climate by excessive emission of CO_2 during the reforming process. The contribution of CO_2 in total greenhouse gas (GHG) emission is 99 wt.% [7]. This excessive amount of CO_2 is the main reason towards the global warming. For the past couple of decades, the burning of the fossil fuels contributes about 75% of CO_2 emission in the atmosphere [8]. In the chemical industries, especially in fired processes, the emission of CO_2 represents a significant contribution to total CO_2 emissions in developed countries. This makes room for a new process, which may be more economical and environmental friendly. To address the issue of global warming, researchers developed a new process known as sorption enhanced steam methane reforming (SE-SMR) process [6, 9-13]. The SE-SMR process works on the principle of hybrid reactor as presented by Mayorga et al. [14]. The hybrid reactor reduces the capital cost of the process as the H_2 producing reactions and much of the H_2 separation

from the product gas take place at the same time in a single reactor [14]. In this way, depending on the end use of the H_2 rich gas product, no separation unit may be required downstream of the process to achieve the desired product purity. In SE-SMR process, CO_2 produced during the global reforming reaction **(R1)** is removed from the reaction zone by the sorption process (**R2**). The removal of CO_2 from the product gases shifts the equilibrium of global reforming reaction **(R1)** towards more H_2 production and enhances the conversion of CH_4.

$$CH_{4(g)} + 2H_2O_{(g)} \leftrightarrow 4H_{2(g)} + CO_{2(g)} \qquad \Delta H^{\circ} = 165\ \text{kJ}\ \ \text{mol}_{CH4}^{-1} \qquad \text{(R1)}$$

Balasubramanian et al. [15] studied the process of CO_2 sorption in the presence of CaO. Thus, the presence of sorbent in the reactor causes the following reaction (**R2**) in the reaction zone;

$$CO_{2(g)} + CaO_{(s)} \leftrightarrow CaCO_{3(s)} \qquad \Delta H^{\circ} = -178.8\ \text{kJ mol}_{CO2}^{-1} \qquad \text{(R2)}$$

The formation of carbonate not only removes the CO_2 from the product stream, it also enhances the production of H_2. This makes the sorption enhanced process a dynamic process in nature. Mayorga et al.[14] listed the potential advantages of SE-SMR process over SMR process.

The concept of SE-SMR is not new. Rostrup-Nielsen [16] proposed the process of hydrocarbon conversion in the presence of steam and Ca-based sorbent. Roger et al. [17] published a patent in which he discussed the process of SMR in the presence of lime as sorbent. Gorin et al. [18] published a patent in which they used fluidized bed reactor for the reforming reactions in the presence of Ca-based sorbent.

In literature, considerable work on SE-SMR is published while considering the fixed bed reactor system. To study the performance of the sorption enhanced process, Balasubramanian et al. [19] used the fixed bed reactor system under high pressure (15 bar) and temperature (650 °C) conditions. They used Ca-based sorbent and observed that 20-25% energy can be saved by using

sorbent in the reforming process as compared to the conventional SMR process. The only disadvantage in the proposed process was the high temperature requirements in the regeneration section. Dou et al. [20] used Ni-based catalyst (5g) and Ca-based sorbent (5g) to study the sorption enhanced steam reforming of glycerol in a packed bed reactor.

Fernández et al. [21] compared CaO and Li_2ZrO_3, K-doped Li_2ZrO_3, Na_2ZrO_3 and Li_4SiO_4 on the basis of the yield of H_2. They reported that using CaO as sorbent makes the overall sorption process in a weakly exothermic, whilst using Li_2ZrO_3 makes the overall reaction weakly endothermic. They derived the optimum conditions for temperature, pressure and S/C to enhance the CH_4 conversion and overall thermal efficiency of the process. It was concluded that CaO gave higher H_2 production as compared to other sorbents such as Li_2ZrO_3, K-doped Li_2ZrO_3, Na_2ZrO_3 and Li_4SiO_4. For the fixed-bed sorption enhanced reactor technology, the stability of CaO is a key issue. The main reasons for the decay of CO_2 capture capacity of CaO are pore blockage and sorbent sintering. However, the study of Alvarez et al. [22] revealed that the pore blockage is negligible for the 100 cycles at shorter carbonation times and sintering remains the main factor of capacity loss.

Fernández et al. [23] developed a mathematical model of Ca/Cu looping process with in situ CO_2 capturing by using CaO as the sorbent in a fixed bed reactor. They studied the effect of S/C, pressure and temperature on the composition of product gases. For the model validation, they used the experimental work of Lee et al. [24]. Koumpouras et al. [25] developed a mathematical model of SE-SMR process in a fixed bed reactor and investigated the effect of sorbent on CH_4 conversion. Ding et al. [26] and Xiu et al. [27] used their own experimental data to validate their developed models of SE-SMR process. In our previous work [28], we developed the SE-SMR model under industrial conditions of temperature and pressure for H_2 production. In the literature, the modelling

of SE-SMR process using CaO as sorbent and NiO/Al_2O_3 as a catalyst under low pressure conditions has not been reported. The applications of medium to low pressure conditions of SE-SMR are relevant to small scale plants or mobile plants, such as those that may be moving from well to well after exhaustion of the first one during shale gas extraction, or such as those that could apply to biogas production at anaerobic digestion plants or wastewater treatment plants. The quality of the hydrogen produced at SE-SMR plants at medium low pressures is superior to that obtained by the same process at conventional SMR plants pressures (28 – 40 bar) because the CH_4 conversion is also much higher. This implies little effort is required in H_2 separation downstream of the process and shows the process in a much better light. To fill this gas, in this paper, one dimensional heterogeneous mathematical model of SE-SMR process is developed and implemented in gPROMS modelbuilder®. The predictions of reactor model are compared with the equilibrium data generated on independent equilibrium-based software (Chemical equilibrium with application software).

2. Mathematical modelling

An adiabatic packed bed reactor, non-ideal plug flow model of the SE-SMR process has been developed using gPROMS. This model accounts for the mass and energy transfer in both gas and solid phase. The assumptions used in this model are the same as used in our previous work [28, 29]. In the present work, different amount of catalyst and sorbent are assumed, but the size of the particles (d_p) is the same.

2.1 Governing equations

On the basis of the assumptions reported in [28], the mathematical equations for mass and energy balances within the reactor filled with sorbent and catalyst particles are listed in **Table 1**. The equations used to calculate the physical properties and model parameters are listed in Abbas et al. [28].

Table 1: Summary of mass and energy balance equations used in the 1-D heterogeneous packed bed reactor model

Mass and energy balances in the gas phase for reforming process;

$$\varepsilon_b\left(\frac{\partial C_i}{\partial t}\right)+\frac{\partial(uC_i)}{\partial z}+k_{g,i}a_v\left(C_i-C_{i,s}\right)=\varepsilon_b D_z\frac{\partial^2 C_i}{\partial z^2} \quad (1)$$

$$\varepsilon_b\rho_g C_{pg}\left(\frac{\partial T}{\partial t}\right)+u\rho_g C_{pg}\frac{\partial(T)}{\partial z}=h_f a_v(T_s-T)+\lambda_z^f\frac{\partial^2 T}{\partial z^2} \quad (2)$$

Where T_s and C_s refer to both catalyst and sorbent particles.

Mass and energy balance in the solid phase;

$$k_{g,i}a_v\left(C_i-C_{i,s}\right)=\upsilon\rho_{cat}r_i-(1-\upsilon)\,\rho_{ads}r_{ads} \quad (3)$$

$$\rho_{bed}C_{p,bed}\left(\frac{\partial T_s}{\partial t}\right)+h_f a_v(T_s-T)+u\rho_{bed}C_{p,bed}\left(\frac{\partial T_s}{\partial z}\right)$$
$$=\upsilon\rho_{cat}\sum-\Delta H_{rxn,j}\,\eta_j R_j+(1-\upsilon)\,\rho_{ads}\sum-\Delta H_{ads}\,r_{ads} \quad (4)$$

Pressure drop calculations across the reactor bed;

$$\frac{\Delta P g_c}{L}=\frac{150}{d_p^2}\left[\frac{(1-\varepsilon)^2}{\varepsilon^3}\right]\mu u+\left(\frac{1.75}{d_p}\right)\left(\frac{1-\varepsilon}{\varepsilon^3}\right)\rho_g u^2 \quad (5)$$

In literature, many expressions have been reported to describe the carbonation kinetics of CaO-based sorbents [23, 24, 30]. Lee et al. [24] performed series of experiments in the temperature range of 650 – 750 °C, they determined the carbonation conversion data. In the past, many efforts were made to describe the kinetics of CO_2 adsorption on the surface of CaO based sorbent [24, 30-32]. Rodriguez et al.[33] proposed a first-order carbonation reaction rate and developed a rate equation for CO_2 adsorption on the surface of CaO sorbent.

$$\frac{dq_{CO2}}{dt} = k_{carb}(X_{max} - X)(\upsilon_{CO2} - \upsilon_{CO2,eq}) \quad (6)$$

Where $\frac{dq_{CO2}}{dt}$ is the rate of adsorption of CO_2 on the surface of adsorbent (r_{ads}, mol $kg^{-1}s^{-1}$) and $\upsilon_{CO2,eq}$ is the volume fraction of CO_2 at equilibrium and it is given as [31];

$$\upsilon_{CO2,eq} = (4.137 \times 10^{7})\exp\left(\frac{-20474}{T}\right) \quad (7)$$

Dedman et al. [34] reported that the carbonation rate of CaO is zero order with respect to CO_2 partial pressure. Bhatia et al.[32] proposed the carbonation rate expression which was independent of partial pressure of CO_2. Lee et al. [24] performed TGA analysis and determined the maximum conversion of active CaO at different temperatures. The experimental data revealed that the conversion of CaO was very low even at a high temperature (750 °C). This may be due to the large size of the CaO particles and low surface area. It was observed that using large size of the pellet, there was no sign of particle deterioration even after many cycles of carbonation and calcination. An expression to calculate the maximum conversion of CaO at any given temperature is given by:

$$X_{max} = 96.34\exp\left(\frac{-12171}{T}\right) 4.49\exp\left(\frac{4790.6}{T}\right) \quad (8)$$

The rate equations, reaction rate constants and equilibrium constants used in this model are given in **Appendix A**.

The reactor model equations (Eqs. 1-4) consist of linear and non-linear partial differential equations (PDEs) and algebraic equations. The initial and boundary conditions used in solving these equations are as follows;

Boundary conditions;

At z = 0

$C_i = C_{i,in}$; $T = T_{in}$; $T_s = T_{s,in}$; $P = P_{in}$

At z = L

$\frac{\partial C_i}{\partial z} = 0$; $\frac{\partial T}{\partial z} = 0$; $\frac{\partial T_s}{\partial z} = 0$

Initial conditions;

$C_i = C_{i,0}$; $T = T_o$; $T_s = T_{s,o}$; $q_{CO2} = 0$

At initial conditions, it was considered that no reactant/product gas, other than N_2, was present within the reactor, so the concentration of gas species was zero at the start i.e. at t = 0. But setting the concentration of H_2 zero made the rates of reforming reactions infinite (A.1-3). To avoid this, a very small initial concentration (~10^{-6}) of the H_2 was used in the solution.

In this work, the BFDM method was used to simulate the reactor model. The overall reactor was divided into 10 – 1000 discretization intervals to check the sensitivity of the model. It was found that the results generated via the gPROMS were not affected by changing the intervals. Finally, the reactor was axially discretized by 100 uniform intervals for this paper and the output results were reported after every second.

3. Results and discussion

In our previous work [28], we validated the SE-SMR fixed bed model by comparing the modelling outputs with the findings of Fernández et al. [23]. The validated model was then tested under the industrial conditions of temperature, pressure, S/C and G_s. In present work, the optimum conditions of temperature, pressure, S/C and G_s for the small scale H_2 production are evaluated. In the following section, the effect of temperature, pressure, S/C and G_s on CH_4 conversion, H_2 yield (wt. % of CH_4), H_2 purity and CO_2 capturing efficiency is simulated. The simulation results obtained using the reactor model are also compared with the equilibrium results generated using CEA software.

The CEA software was used to generate the equilibrium data [35, 36]. This software is based on minimization of Gibbs free energy (G) [37, 38]. The chemical equilibrium analysis was done by considering the gas species involved in the reactant and product streams, which are CH_4, H_2, CO, CO_2, H_2O, N_2, CaO and $CaCO_3$, using the option 'ONLY' in CEA. This allows specification of a restricted pool of species as potential equilibrium products. The calculations of individual equilibrium molar outputs were performed on the basis of N_2 balance, which allowed the determination of the total moles of product at equilibrium in post processing, and its product with the relevant mole fractions predicted by the CEA output. The solid carbon equilibrium product was not included as it is not significant in conditions of excess stoichiometric steam of the present study. To study the effect of temperature, pressure and S/C were fixed and the CEA code runs in temperature-pressure (tp) mode, corresponding to an isothermal and isobaric process. Similarly, to study the pressure effect; temperature and S/C conditions were fixed, still in tp mode.

3.1 Effect of temperature

In **Figure 1**, the fixed bed model at constant pressure of 3 bar, S/C of 3.0, and 3.5 kg $m^{-2}s^{-1}$ generated CH_4 conversions between 19.6 and 88% with a rise in temperature from 400 to 750 °C, whilst the H_2 yield (wt. % of CH_4), increased from 7.5 to 37%. The equilibrium data of CH_4 conversion and H_2 yield (wt. % of CH_4) predicted using CEA, under the same operating conditions, was 59 – 95% and 30 – 43% respectively in agreement with the endothermic in nature of the process and the high temperature favouring the overall SMR process. As the temperature rose from 650 °C (923 K), the increase in CH_4 conversion and H_2 yield was negligible. The fixed bed, initially away from equilibrium at 400 °C, progressively approached equilibrium as the temperature increased from 500 – 750 °C the modelling results approach the equilibrium values of CH_4 conversion and H_2 yield (wt. % of CH_4).

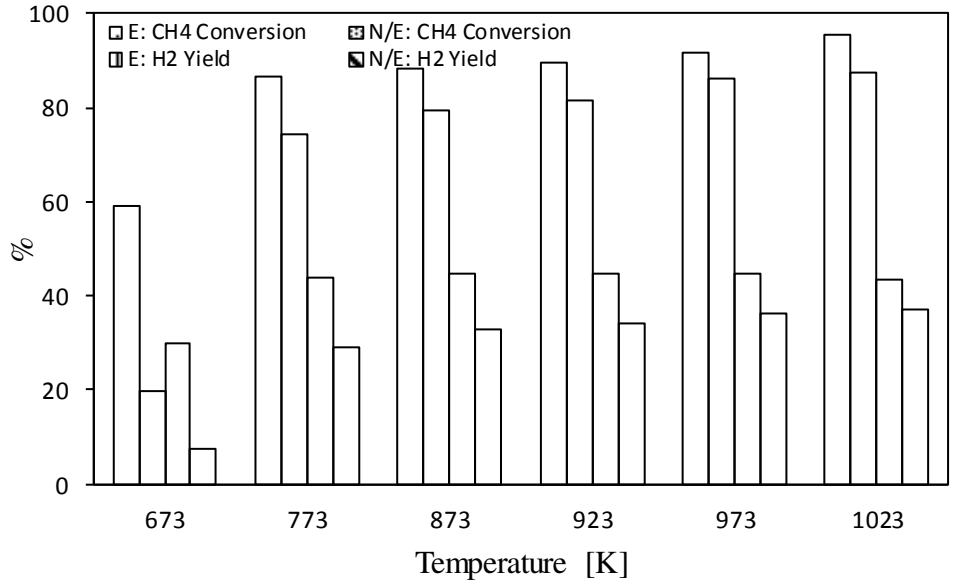

Figure 1: The effect of temperature on the CH_4 conversion and H_2 yield (wt. % of CH_4) at 3 bar, S/C of 3.0, CaO/C of 1.0 and gas mass flow velocity of 3.5 kg $m^{-2}s^{-1}$ (E: Equilibrium and N/E: Non-Equilibrium or Modelling results for the fixed bed)

Figure 2 illustrates the effect of temperature on H_2 purity and CO_2 capture efficiency of the fixed bed under the conditions of 3 bar, S/C of 3 and 3.5 kg $m^{-2}s^{-1}$. The CO_2 capture efficiency is calculated by using Eq. 9.

$$CO_2 \text{capture efficiency } (\%) = \frac{\left(n_{CH4,i} - n_{CH4,o} - n_{CO,o} - n_{CO2,o}\right)}{n_{CH4,i}} \times 100 \quad (9)$$

It can be seen for the fixed bed in non-equilibrium that CO_2 capture efficiency increased from 19 to 66% as temperature increased from 400 to 500 °C compared to equilibrium values rising from 59 to 86%. As temperature increased from 500 – 750 °C, the CO_2 capture efficiency, in both modelling and equilibrium cases, decreased from 66 to 33.5% and from 86 to 35%, respectively. This drop in CO_2 capture efficiency resulted in a decrease in H_2 purity at the outlet of the reactor. The purity of H_2 declined from 87 – 81% and 96 – 84% as temperature rose from 500 – 750 °C for the non-equilibrium fixed bed and the equilibrium conditions, respectively. As adsorption of CO_2 is an exothermic reaction, hence low temperature favours this reaction. At high temperature (600 – 750 °C), the adsorption reaction is not favourable, and it makes more CO_2 at the outlet of the reactor eventually results in low H_2 purity.

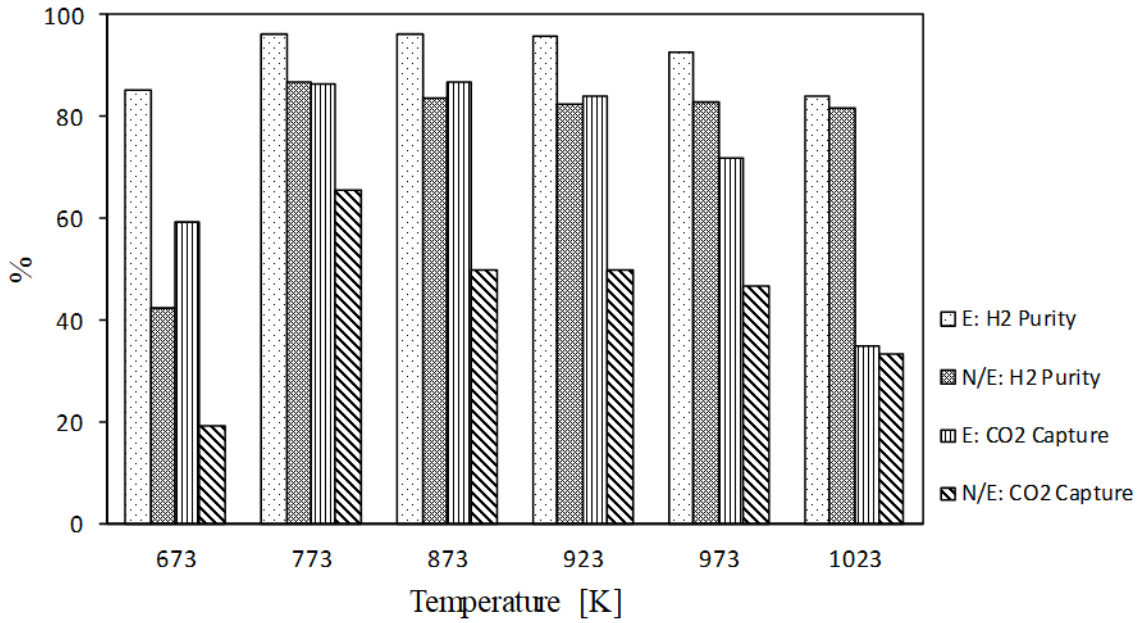

Figure 2: The effect of temperature on the H_2 purity and CO_2 capture efficiency at 3bar, S/C of 3.0, CaO/C of 1.0 and gas mass flow velocity of 3.5 kg $m^{-2}s^{-1}$

Figure 3 shows the effect of temperature on the thermal efficiency of the SE-SMR process. The thermal efficiency is calculated using Eq. 10.

$$\text{Thermal efficiency } [\%] = \frac{(\text{moles of } H_2 \text{ at outlet}) \times (\text{LHV}_{H2})}{(\text{moles of } CH_4 \text{ at intlet}) \times (\text{LHV}_{CH4})} \times 100 \qquad (10)$$

The increase in temperature favours the reforming process hence more production of H_2 at the outlet of the reactor results in increase in the thermal efficiency of the process. The rise in thermal efficiency was 18 – 95% as temperature increased from 400 – 750 °C. Beyond 650 °C, the rise in thermal efficiency was almost negligible. Thus, the optimum temperature for SE-SMR process under the conditions of 3 bar, S/C of 3 and 3.5 kg $m^{-2}s^{-1}$ was 650 °C (923 K).

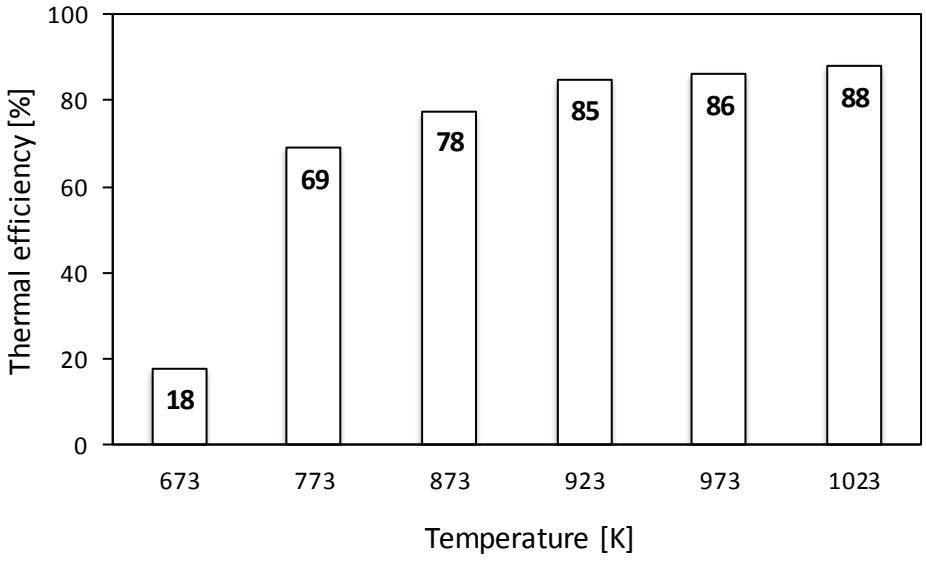

Figure 3: The effect of temperature on the thermal efficiency of reforming process at 3 bar, S/C of 3.0, CaO/C of 1.0 and gas mass flow velocity of 3.5 kg $m^{-2}s^{-1}$

3.2 Effect of pressure

Pressure plays a vital role in the reforming process. According to Le-Chatelier's principle, pressure has a negative equilibrium effect on hydrogen production by steam reforming. This is due to the non-zero stoichiometric molar balance between the gas products and reactants in reaction R1 (5 moles gas products vs. 3 moles gas reactants). Reaction R1 reduces but does not eliminate this molar gas imbalance, which pitches 5 moles of gas product against 3 moles of gas reactants. As pressure increases from one equilibrium to another, Le Chatelier's principle will counteract the rise in pressure by favouring reactants with the lower partial pressures due to their lower molar concentration.

In the previous section, 923 K was selected as an optimum temperature. So, the effect of pressure on the SE-SMR is studied at this constant temperature. In **Figure 4**, the effect of pressure on CH_4

conversion and H_2 yield (in wt. % of CH_4) at 650 °C, S/C of 3 and 3.5 kg $m^{-2}s^{-1}$ is illustrated. As expected from the equilibrium trend, the rise in pressure has a negative effect on CH_4 conversion and H_2 yield (wt. % of CH_4). At equilibrium, the CH_4 conversion dropped from 92 to 83% as pressure increased from 2 to 7 bar, while H_2 yield decreased from 46 to 42 wt.% of CH_4 feed. In the fixed bed model, the same pressure increase induced more significant drops in both CH_4 conversion from 91 to 78% and H_2 yield from 38 to 32 wt.%.

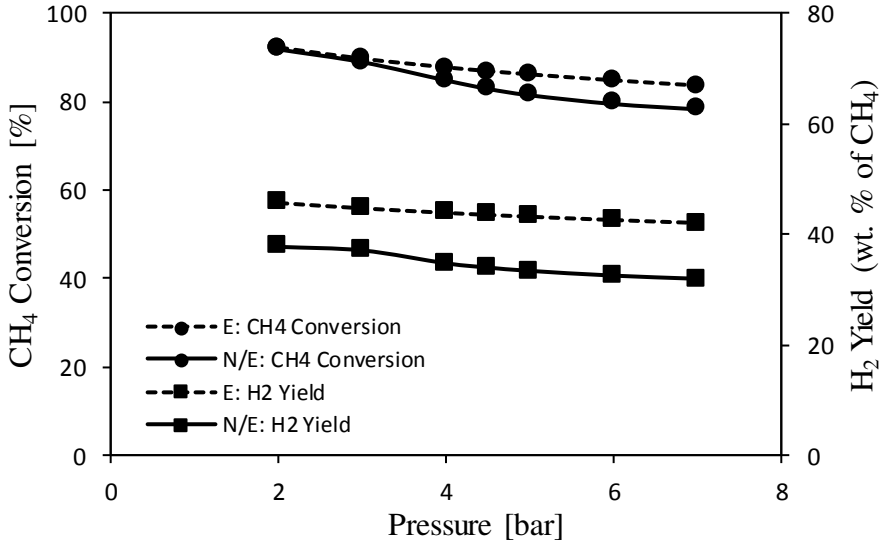

Figure 4: The effect of pressure on the CH_4 conversion and H_2 yield (wt. % of CH_4) at 923 K, S/C of 3.0, CaO/C of 1.0 and gas mass flow velocity of 3.5 kg $m^{-2}s^{-1}$

Figure 5 shows the effect of pressure on H_2 purity and CO_2 capture efficiency. The CO_2 capture efficiency decreased weakly for a 2 to 7 bar change in pressure. In the fixed bed model, the drop was from 53 to 51%, and at equilibrium, from 83 to 81%. Simultaneously, H_2 purity decreased from 96 to 95% at equilibrium, and from 86 to 84% for the fixed bed case. The rate of CO_2 adsorption reaction is high at low pressures as reforming reaction is favourable at low pressures and resulted in more CO_2 at the outlet than high pressures.

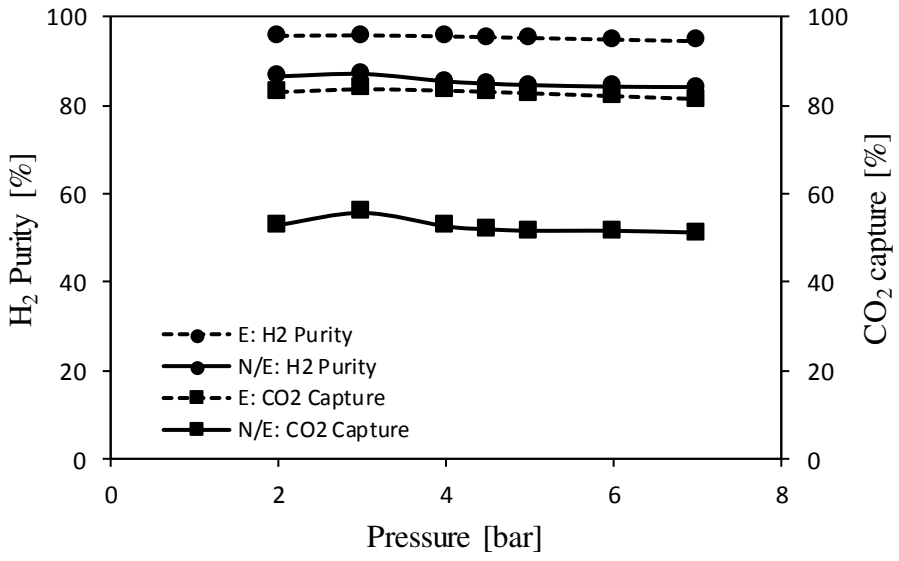

Figure 5: The effect of pressure on the H_2 purity and CO_2 capture efficiency at 923 K, S/C of 3.0, CaO/C of 1.0 and gas mass flow velocity of 3.5 kg $m^{-2}s^{-1}$

In **Figure 6**, the dynamic profile of rate of carbonation reaction for 2 – 7 bar conditions at 923 K, S/C of 3, 3.5 kg $m^{-2}s^{-1}$ gas mass flow velocity confirmed that the carbonation rate is higher at low pressures than high pressure conditions. The maximum carbonation rate was observed at 2 bar which is nearly twice the rate of carbonation reaction at 7 bar.

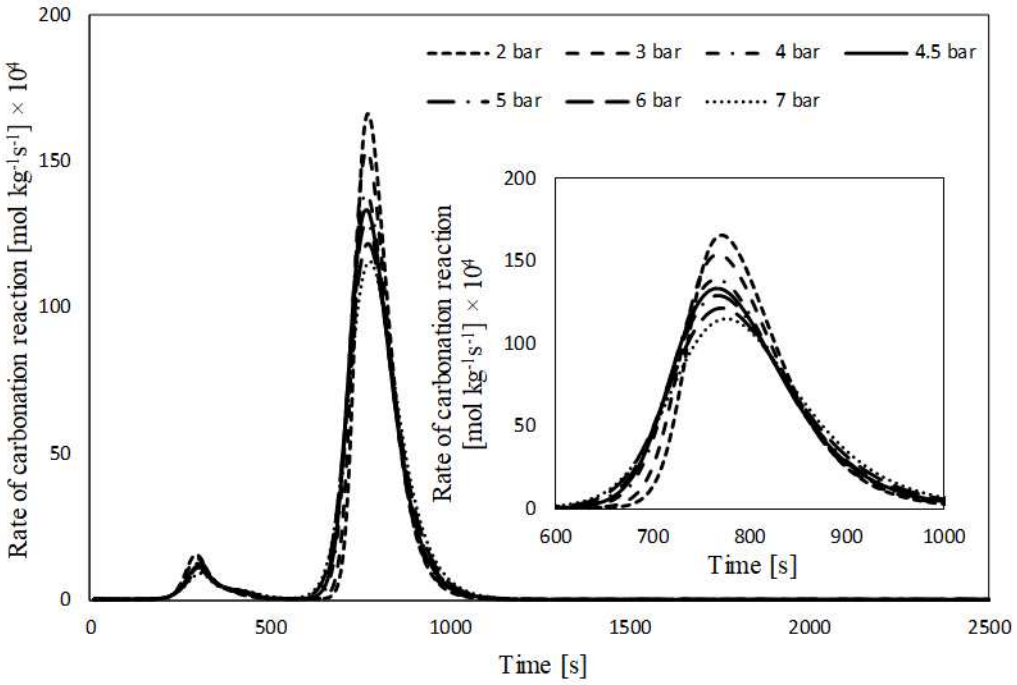

Figure 6: The effect of pressure on the rate of carbonation at 923 K, S/C of 3.0, CaO/C of 1.0 and gas mass flow velocity of 3.5 kg $m^{-2}s^{-1}$

The optimum pressure for the SE-SMR process is found to be 3 bar under the conditions of 923 K, S/C of 3 and 3.5 kg $m^{-2}s^{-1}$ gas mass flow velocity.

3.3 Effect of S/C

The amount of steam feed used in the steam reforming process determines the overall conversion of the fuel and yield of H_2. The stoichiometric S/C for SE-SMR process is 2. In practice, the amount of steam higher than stoichiometric ratio favours more conversion of CH_4 into the desired hydrogen product as it reduces the chances of carbon deposition on the surface of the catalyst particles. The effect of S/C on the conversion of CH_4, H_2 yield (wt. % of CH_4), H_2 purity, CO_2 capture efficiency and thermal efficiency is shown in **Table 2**.

Table 2: Effect of S/C on the CH_4 conversion, H_2 yield (wt. % of CH_4), H_2, CO_2 capture efficiency and thermal efficiency at 923 K, 3 bar and gas mass flow velocity of 3.5 kg $m^{-2}s^{-1}$

S/C [-]	**CH_4 conv [%]**	**H_2 yield (wt.% CH_4)**	**H_2 Purity [%]**	**CO_2 capture efficiency [%]**	**Thermal efficiency (%)**
1	E: 45.2 N/E: 44.5	E: 21.9 N/E: 17.9	E: 73.2 N/E: 65.0	E: 35.6 N/E: 23.6	E: 52.1 N/E: 42.6
2	E: 73.5 N/E: 69.8	E: 36.5 N/E: 28.7	E: 89.7 N/E: 78.2	E: 66.8 N/E: 36.8	E: 86.8 N/E: 68.1
3	E: 89.6 N/E: 89.4	E: 44.8 N/E: 35.7	E: 95.63 N/E: 84.9	E: 83.78 N/E: 49.6	E: 100 N/E: 84.8
4	E: 95.9 N/E: 92.1	E: 48.1 N/E: 38.5	E: 97.6 N/E: 86.6	E: 90.6 N/E: 52.9	E: 100 N/E: 91.5
5	E: 98.1 N/E: 96.7	E: 49.3 N/E: 40.7	E: 98.2 N/E: 88.1	E: 92.9 N/E: 56.6	E: 100 N/E: 96.7

As the S/C rose from 1 to 5, the conversion of CH_4 increased drastically from 45 to 98% at equilibrium and from 44 to 97% in the fixed bed. Similarly, the H_2 purity increased from 73 to 98% at equilibrium and from 65 to 88% in the fixed bed. The effect of S/C on H_2 yield was negligible as S/C increased beyond 3. It is also clear from the results that more steam had the effect of enhancing the purity of H_2. It is concluded from the results that higher S/C results in higher purity of H_2, CH_4 conversion and H_2 yield although this would reduce the overall process cost as more heat is required for the generation of the excess steam. The optimum S/C of 3 was selected under the operating conditions of 923 K and 3 bar.

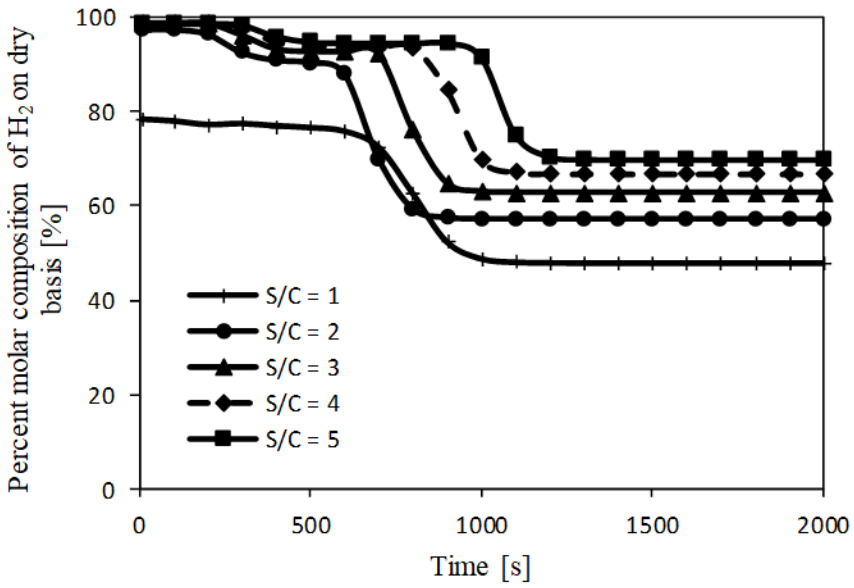

Figure 7: The effect of S/C on the molar composition of H_2 (dry basis) at 923 K, 3 bar, CaO/C of 1.0 and gas mass flow velocity of 3.5 kg $m^{-2}s^{-1}$

In **Figure 7**, the dynamic profile of molar composition of H_2 (dry basis) under the operating conditions of 923 K, 3 bar, 3.5 kg $m^{-2}s^{-1}$ gas mass flow velocity is presented for S/C in the range 1 – 5. It can be seen as the S/C increased the purity of H_2 produced at the exit of the reactor increased. The effect on H_2 production (molar percent) was negligible after the S/C of 3. This behaviour is confirmed in **Figure 8** which plots the rate of the global SMR reaction was higher for the higher S/C as more steam is available for the reforming reaction hence more H_2 is produced.

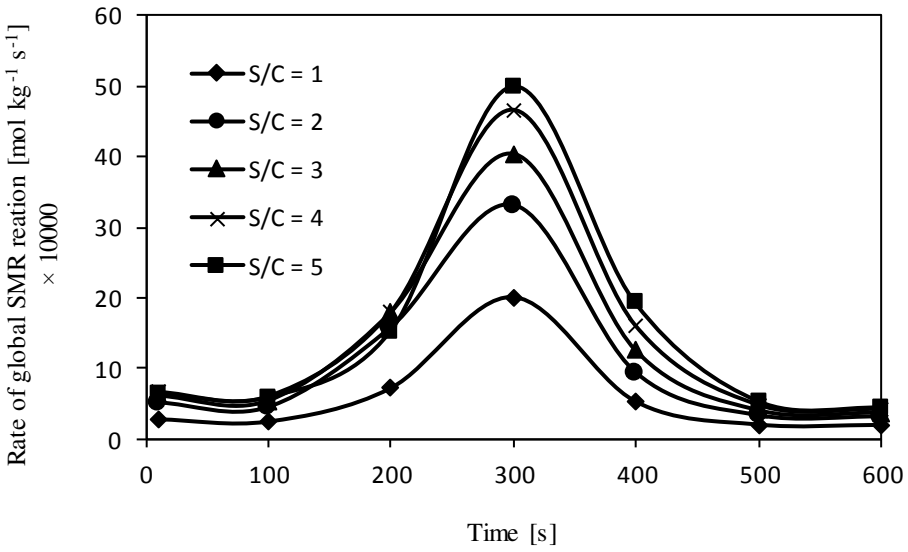

Figure 8: The effect of S/C on the reaction rate of global SMR at 923 K, 3 bar, CaO/C of 1.0 and gas mass flow velocity of 3.5 kg $m^{-2}s^{-1}$

3.4 Effect of gas mass flow velocity (Gs)

The gas mass flow velocity (G_s) is another important operating variable that affects the performance of the system. The selection of G_s is highly dependent upon the length of the reactor. Rostrup et al.[39] proposed 1.5 – 2 m s^{-1} velocity as the optimum velocity to get the conversion of CH_4 close to the equilibrium conditions.

In this work, various values of G_s are used to study the effect on the performance of the SE-SMR process. In **Figure 9**, the dynamic variation of CO_2 and H_2 composition (dry basis) is presented under the operating conditions of 923 K, 3 bar, S/C of 3.0 and various G_s from 1 to 4.5 kg m^{-2} s^{-1}. The lower G_s resulted in a longer pre-breakthrough period as the residence time was higher in the reactor and a higher conversion of CH_4 was achieved. As G_s increased, the CH_4 conversion decreased because of shorter residence time. The longer pre-breakthrough periods for lower G_s may be unsuitable for fast cyclic processes. The pre-breakthrough period increased from 500 s to

1300 s as G_s decreased from 4.5 kg $m^{-2}s^{-1}$ to 1 kg $m^{-2}s^{-1}$. The optimum G_s selected was 3.5 kg $m^{-2}s^{-1}$ due to having a pre-breakthrough period of 600s. At this G_s, CH_4 conversion and H_2 purity were 99% and 95% respectively.

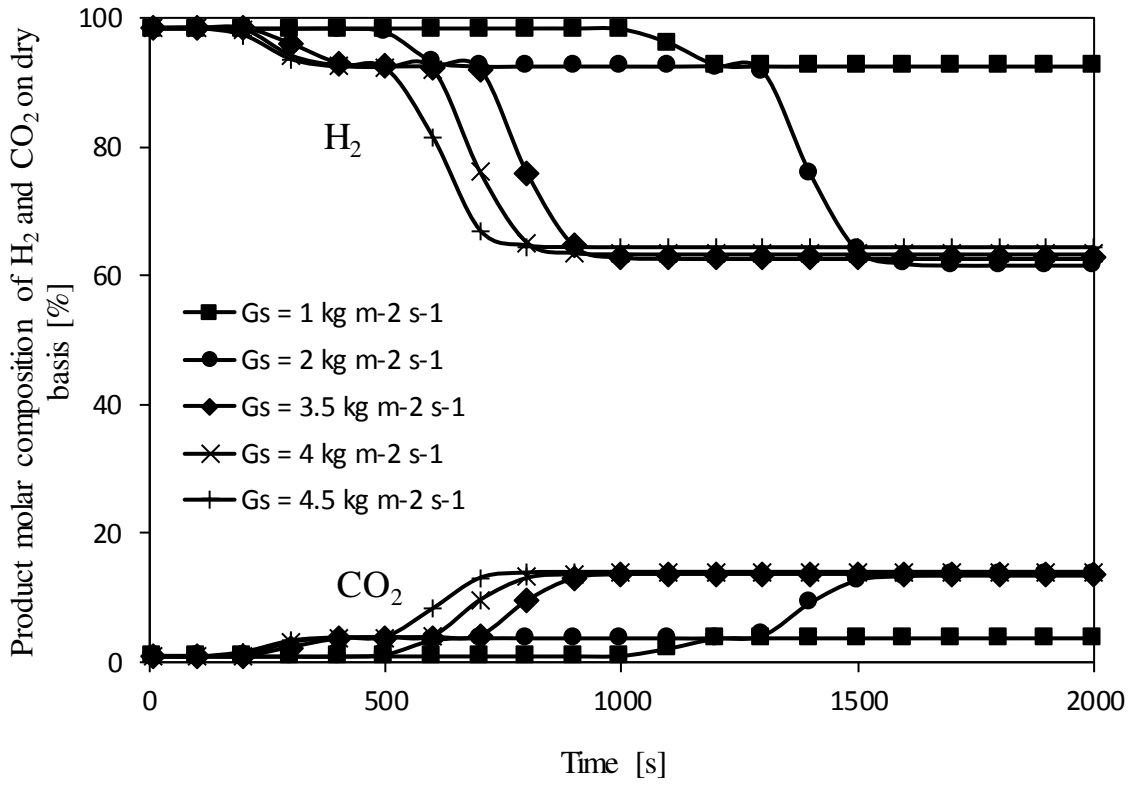

Figure 9: Dynamic profile of H_2 and CO_2 composition (dry basis) at the outlet of reactor for various G_s under the adiabatic conditions, at 923K, 3bar and S/C of 3.0

3.5 Comparison of SMR and SE-SMR process

In this section, the performance of developed model SE-SMR reactor is compared with the performance of conventional SMR reactor model in terms of conversion enhancement of CH_4. The CH_4 conversion enhancement is calculated by using Eq. 11.

$$CH_4 \text{conversion enhancement } (\%) = \frac{\left(X_{CH4,nad} - X_{CH4,ad}\right)}{X_{CH4,nad}} \times 100 \quad (11)$$

Figure 10 shows the advantage of using sorbent in a packed bed reactor along with the catalysts during reforming process. A conversion enhancement of 87% was observed at 600 s. This point was the time period at which sorbent was fully active and working at its full capacity. After 600 s, a decrease in conversion enhancement was observed. This was the period when sorbent was getting saturated and no more active site of sorbent was available for the further adsorption of CO_2. Ultimately, after 900 s, there was no CH_4 conversion enhancement. This is due to the fact that after 900 s, the carbonation rate is zero and the SE-SMR process behaves like conventional SMR.

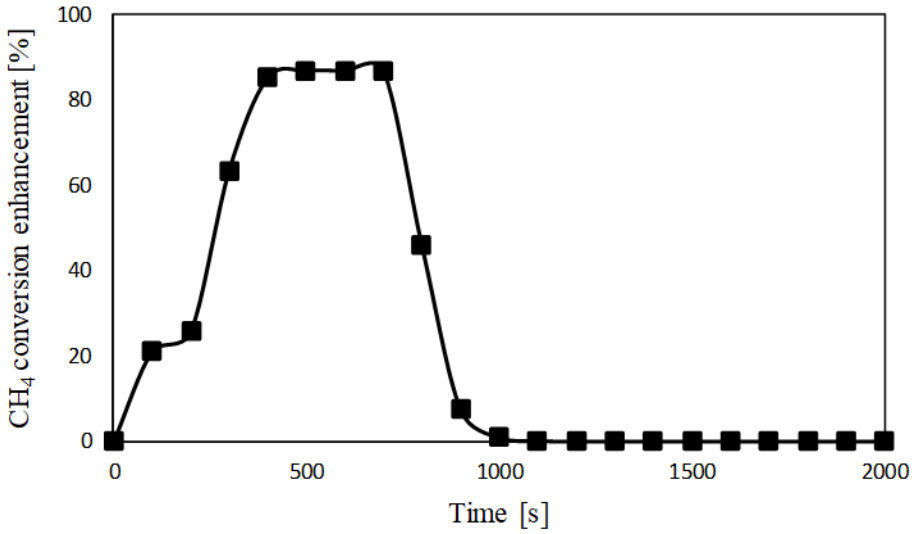

Figure 10: Dynamic variation of CH_4 conversion enhancement under the adiabatic conditions, at 923K, 3 bar, S/C of 3.0 and 3.5 kg $m^{-2}s^{-1}$ gas mass flow velocity

4. Conclusion

The developed 1-dimensional model of SE-SMR reactor was tested under the low-pressure conditions (2 – 7 bar) compatible with small-scale production of H_2. The performance of the SE-SMR reactor was studied in terms of CH_4 conversion, H_2 purity and yield, and the capturing

efficiency of the CO_2. It is concluded that the selection of temperature for a small scale H_2 production, via SE-SMR, is a trade-off between the conversion of CH_4 and H_2 purity. The high temperature is favourable for the CH_4 conversion but at temperature higher than 923 K, the carbonation reaction (R2) is not favourable and resulted in more CO_2 at the outlet of reactor which resulted in decreasing the purity of H_2. At 923 K, the CH_4 conversion and H_2 purity achieved were 89 % and 87% respectively under the operating pressure of 3 bar, S/C of 3 and G_s of 3.5 kg $m^{-2}s^{-1}$. The increase in operating pressure caused a decrease in CH_4 conversion, hence the yield of H_2 also decreased. A pressure of 3 bar was selected as the optimum pressure in this study. At 3 bar, 923 K, S/C of 3 and G_s of 3.5 kg $m^{-2}s^{-1}$, the CO_2 capture efficiency was 56%. This capture efficiency decreased with further increase in the pressure. A S/C of 3 and G_s of 3.5 kg m^{-2} s^{-1} was selected as an optimum value in this study. The overall CH_4 conversion enhancement obtained in SE-SMR process under the optimum operating conditions of temperature, pressure S/C and G_s was 87% as compared to the conventional SMR process.

Acknowledgment

The following are gratefully acknowledged: The support of University of Engineering and technology (UET) Lahore, Pakistan, Dr. Feng Cheng for help with CEA modelling, and C2-181 project grant to the University of Leeds via UKRI's UKCCSRC's consortium grant EP/K000446/1, UK for funding the licence of gPROMS.

NOMENCLATURE

a_v	Interfacial area per unit volume of catalyst bed, m^2/m^3
C_i	Concentration of component i, mol/m^3
$C_{i,in}$	Inlet concentration of component i, mol/m^3
$C_{i,o}$	Concentration of component i at t=0, mol/m^3
$C_{i,s}$	Concentration of component i on solid surface, mol/m^3
C_{pg}	Heat capacity of gas at constant pressure, J/(kg.K)
$C_{p,bed}$	Heat capacity of bed at constant pressure, J/(kg.K)
D_m	Average molecular diffusivity, m^2/s
d_P	Catalyst particle diameter, m
D_z	Axial dispersion coefficient, m^2/s
E_j	Activation energy of reaction j, J/mol
G_s	Gas mass flow velocity, $kg/(m^2.s)$
h_f	Gas to solid heat transfer coefficient, $W/(m^2.s)$
$k_{g,i}$	Gas to solid mass transfer coefficient of component i, m^3/m^2s
K_i	Adsorption constant of species i, bar^{-1}
k_j	Kinetic rate constant of reaction j, (mol/ (kgcat s))
$K_{o,i}$	Reference adsorption constant of species i, bar^{-1}
K_j	Thermodynamic equilibrium constant of reaction j, bar^2
k_z	Axial thermal conductivity, W/(m.K)
L	Packed bed length, m
p_i	Partial pressure of specie i, bar
P	Total pressure, bar

p_i^{feed}	Partial pressure of component i in feed, bar
P^o	Pressure at z=0, bar
P_{in}	Inlet pressure of the feed, bar
q_{CO2}	Solid phase concentration of CO_2 (average on the surface of sorbent), mol/m^3
R, R_g	Ideal gas constant, J/(mol.K)
r_i	Rate of production of component i, $mol/(kg_{cat}.s)$
r_{ads}	Rate of adsorption of CO_2, mol/(kg.s)
R_j	Rate of reaction j, $mol/(kg_{cat}.s)$
T	Temperature within system, K
T_{in}	Inlet temperature, K
T_s	Temperature of catalyst particles, K
$T_{s,o}$	Temperature of solid particles at 't=0', K
T_w	Wall temperature, K
u_s, v	Superficial velocity, m/s
X_{max}	Maximum fractional carbonation conversion of CaO
X_{CH4}	Fractional conversion of CH_4
$X_{CH4, ad}$	Fractional conversion of CH_4 with adsorbent
$X_{CH4, nad}$	Fractional conversion of CH_4 without adsorbent
ΔH_{rex}	Heat of reaction at standard condition, J/mol
ΔH_{ads}	Heat of adsorption reaction at standard condition, J/mol
ΔP	Pressure drop across the reactor, bar
Greek letters	

Ω	Denominator term in the reaction kinetics
λ_z^f	Effective thermal conductivity, W/(m.K)
ρ_f	Density of fluid, kg/m^3
ρ_{cat}	Density of catalyst, kg/m^3
ρ_{ad}	Density of sorbent, kg/m^3
η_j	Effectiveness factor of reaction 'j'
Φ_{ij}	Stoichiometric coefficient of component 'i' in reaction 'j'
μ_g	Viscosity of gas, Pa.s
υ	Ratio of catalyst amount to sorbent amount

APPENDIX A

The kinetic rate equations and kinetic data used for this modelling work are given as [40];

$$R_{SMR} = \frac{k_{SMR}}{p_{H_2}^{2.5}}\left(p_{CH_4}p_{H_2O} - \frac{p_{H_2}^3 p_{CO}}{K_{SMR}}\right)\left(\frac{1}{\Omega^2}\right) \quad (A.1)$$

$$R_{WGS} = \frac{k_{WGS}}{p_{H_2}}p_{CO}p_{H_2O} - \frac{p_{H_2}p_{CO_2}}{K_{WGS}}\left(\frac{1}{\Omega^2}\right) \quad (A.2)$$

$$R_{Global\ SMR} = \frac{k_{Global\ SMR}}{p_{H_2}^{3.5}}\left(p_{CH_4}p_{H_2O}^2 - \frac{p_{H_2}^4 p_{CO_2}}{K_{global\ SMR}}\right)\left(\frac{1}{\Omega^2}\right) \quad (A.3)$$

$$k_{SMR} = k_{0,SMR}\exp\left(\frac{-E_{SMR}}{RT}\right) = (1.17 \times 10^{15})\exp\left(\frac{-240100}{RT}\right) \quad (A.4)$$

$$k_{WGS} = k_{0,WGS}\exp\left(\frac{-E_{WGS}}{RT}\right) = (5.43 \times 10^{5})\exp\left(\frac{-67130}{RT}\right) \quad (A.5)$$

$$k_{Global\ SMR} = k_{0,Global\ SMR}\exp\left(\frac{-E_{Global\ SMR}}{RT}\right) = (2.83 \times 10^{14})\exp\left(\frac{-243900}{RT}\right) \quad (A.6)$$

$$K_{SMR} = \exp\left(\frac{-26830}{T_s} + 30.114\right) \quad (A.7)$$

$$K_{WGS} = \exp\left(\frac{4400}{T_s} - 4.036\right) \quad (A.8)$$

$$K_{Global\ SMR} = K_{SMR}K_{WGS} \quad (A.9)$$

$$\Omega = 1 + K_{CO}p_{CO} + K_{H_2}p_{H_2} + K_{CH_4}p_{CH_4} + K_{H_2O}\frac{p_{H_2O}}{p_{H_2}} \quad (A.10)$$

$$K_i = K_{oi}\exp\left(\frac{-\Delta H_i}{R_g T}\right) \quad (A.11)$$

REFERENCES

[1] Badwal SP, Giddey S, Munnings C. Hydrogen production via solid electrolytic routes. Wiley Interdisciplinary Reviews: Energy and Environment. 2013;2:473-87.

[2] Rostrup-Nielsen JR. Production of synthesis gas. Catalysis today. 1993;18:305-24.

[3] Oliveira EL, Grande CA, Rodrigues AE. Steam methane reforming in a Ni/Al2O3 catalyst: kinetics and diffusional limitations in extrudates. The Canadian Journal of Chemical Engineering. 2009;87:945-56.

[4] Abbas S, Dupont V, Mahmud T. Kinetics study and modelling of steam methane reforming process over a NiO/Al2O3 catalyst in an adiabatic packed bed reactor. International Journal of Hydrogen Energy. 2017;42:2889-903.

[5] Oliveira EL, Grande CA, Rodrigues AE. Methane steam reforming in large pore catalyst. Chemical Engineering Science. 2010;65:1539-50.

[6] Bartholomew CH, Farrauto RJ. Fundamentals of industrial catalytic processes: John Wiley & Sons; 2011.

[7] Barelli L, Bidini G, Gallorini F, Servili S. Hydrogen production through sorption-enhanced steam methane reforming and membrane technology: a review. Energy. 2008;33:554-70.

[8] Metz B, Davidson O, De Coninck H, Loos M, Meyer L. IPCC special report on carbon dioxide capture and storage. Prepared by Working Group III of the Intergovernmental Panel on Climate Change. IPCC, Cambridge University Press: Cambridge, United Kingdom and New York, USA. 2005;4.

[9] Xiu G-h, Li P, Rodrigues AE. Sorption-enhanced reaction process with reactive regeneration. Chemical engineering science. 2002;57:3893-908.

[10] Harrison DP. Sorption-enhanced hydrogen production: a review. Industrial & engineering chemistry research. 2008;47:6486-501.

[11] Rodrigues AE, Madeira LM, Wu Y-J, Faria R. Sorption-enhanced Reaction Processes: World Scientific; 2018.

[12] Chanburanasiri N, Ribeiro AM, Rodrigues AE, Arpornwichanop A, Laosiripojana N, Praserthdam P, et al. Hydrogen production via sorption enhanced steam methane reforming process using Ni/CaO multifunctional catalyst. Industrial & Engineering Chemistry Research. 2011;50:13662-71.

[13] Wang Y-N, Rodrigues AE. Hydrogen production from steam methane reforming coupled with in situ CO2 capture: conceptual parametric study. Fuel. 2005;84:1778-89.

[14] Mayorga SG, Hufton JR, Sircar S, Gaffney TR. Sorption enhanced reaction process for production of hydrogen. Phase 1 final report. Air Products and Chemicals, Inc., Allentown, PA (United States); 1997.

[15] Balasubramanian B, Ortiz AL, Kaytakoglu S, Harrison D. Hydrogen from methane in a single-step process. Chemical Engineering Science. 1999;54:3543-52.

[16] Rostrup-Nielsen JR. Catalytic steam reforming: Springer; 1984.

[17] Roger W. Hydrogen production. Google Patents; 1933.

[18] Retallick WB. Method for the production of hydrogen. Google Patents; 1963.

[19] Balasubramanian B, Lopez Ortiz A, Kaytakoglu S, Harrison D. Hydrogen from methane in a single-step process. Chemical Engineering Science. 1999;54:3543-52.

[20] Dou B, Rickett GL, Dupont V, Williams PT, Chen H, Ding Y, et al. Steam reforming of crude glycerol with in situ CO 2 sorption. Bioresource Technology. 2010;101:2436-42.

[21] Ochoa-Fernández E, Haugen G, Zhao T, Rønning M, Aartun I, Børresen B, et al. Process design simulation of H 2 production by sorption enhanced steam methane reforming: evaluation of potential CO 2 acceptors. Green Chemistry. 2007;9:654-62.

[22] Alvarez D, Abanades JC. Determination of the critical product layer thickness in the reaction of CaO with CO2. Industrial & engineering chemistry research. 2005;44:5608-15.

[23] Fernandez J, Abanades J, Murillo R. Modeling of sorption enhanced steam methane reforming in an adiabatic fixed bed reactor. Chemical Engineering Science. 2012;84:1-11.

[24] Lee DK, Baek IH, Yoon WL. Modeling and simulation for the methane steam reforming enhanced by in situ CO 2 removal utilizing the CaO carbonation for H 2 production. Chemical Engineering Science. 2004;59:931-42.

[25] Koumpouras GC, Alpay E, Stepanek F. Mathematical modelling of low-temperature hydrogen production with in situ CO< sub> 2</sub> capture. Chemical Engineering Science. 2007;62:2833-41.

[26] Ding Y, Alpay E. Adsorption-enhanced steam–methane reforming. Chemical Engineering Science. 2000;55:3929-40.

[27] Xiu G, Li P, Rodrigues AE. Adsorption-enhanced steam-methane reforming with intraparticle-diffusion limitations. Chemical Engineering Journal. 2003;95:83-93.

[28] Abbas S, Dupont V, Mahmud T. Modelling of H 2 production in a packed bed reactor via sorption enhanced steam methane reforming process. International Journal of Hydrogen Energy. 2017.

[29] Abbas S, Dupont V, Mahmud T. Modelling of high purity H2 production via sorption enhanced chemical looping steam reforming of methane in a packed bed reactor. Fuel. 2017;202:271-86.

[30] Li Z-s, Cai N-s. Modeling of multiple cycles for sorption-enhanced steam methane reforming and sorbent regeneration in fixed bed reactor. Energy & Fuels. 2007;21:2909-18.

[31] Baker E. 87. The calcium oxide–carbon dioxide system in the pressure range 1—300 atmospheres. Journal of the Chemical Society (Resumed). 1962:464-70.

[32] Bhatia S, Perlmutter D. Effect of the product layer on the kinetics of the CO2- lime reaction. AIChE Journal. 1983;29:79-86.

[33] Rodríguez N, Alonso M, Abanades J. Experimental investigation of a circulating fluidized-bed reactor to capture CO2 with CaO. AIChE Journal. 2011;57:1356-66.

[34] Dedman A, Owen A. Calcium cyanamide synthesis. Part 4.—The reaction CaO+ CO 2= CaCo 3. Transactions of the Faraday Society. 1962;58:2027-35.

[35] McBride BJ, Gordon S. Computer Program for Calculation of Complex Chemical Equilibrium Compositions and Applications: II: Nationa Aeronautics and Space Administration, Office of Management, Scientific and Technical Information Program; 1996.

[36] Kee RJ, Rupley FM, Miller JA. Chemkin-II: A Fortran chemical kinetics package for the analysis of gas-phase chemical kinetics. Sandia National Labs., Livermore, CA (USA); 1989.

[37] Adiya ZIS, Dupont V, Mahmud T. Chemical equilibrium analysis of hydrogen production from shale gas using sorption enhanced chemical looping steam reforming. Fuel Processing Technology. 2017;159:128-44.

[38] Adiya ZIS, Dupont V, Mahmud T. Effect of hydrocarbon fractions, N2 and CO2 in feed gas on hydrogen production using sorption enhanced steam reforming: Thermodynamic analysis. international journal of hydrogen energy. 2017;42:21704-18.

[39] Rostrup-Nielsen J, Sehested J, Nørskov JK. Hydrogen and synthesis gas by steam-and CO 2 reforming. Advances in Catalysis2002.

[40] Abbas S, Dupont V, Mahmud T. Modelling of H2 production in a packed bed reactor via sorption enhanced steam methane reforming process. International journal of hydrogen energy. 2017;42:18910-21.